Compartmentalization of Central Neurons in *Drosophila*: A New Strategy of Mosaic Analysis Reveals Localization of Presynaptic Sites to Specific Segments of Neurites

Robert Löhr,[1] Tanja Godenschwege,[2] Erich Buchner,[3] and Andreas Prokop[1]

[1]Institute of Genetics, University of Mainz, D-55128 Mainz, Germany, [2]Department of Biology, University of Massachusetts, Amherst Massachusetts 01003, and [3]Biocentre of the University, D-97074 Würzburg, Germany

Synaptogenesis in the CNS has received far less attention than the development of neuromuscular synapses, although only central synapses allow the study of neuronal postsynaptic mechanisms and display a greater variety of structural and functional features. This neglect is attributable mainly to the enormous complexity of the CNS, which makes the visualization of individual synapses on defined neuronal processes very difficult. We overcome this obstacle and demonstrate by confocal microscopy the specific arrangement of output synapses on individual neurites. These studies are performed via genetic mosaic strategies in the CNS of the fruitfly *Drosophila melanogaster*. First, we use targeted expression of synaptic proteins by the UAS/Gal4 system. Second, we apply a newly developed transplantation-based mosaic strategy that takes advantage of the intrinsic regulation and localization of synaptic proteins in single-cell clones. We propose the existence of three distinct neuritic compartments: (1) primary neurites that appear to form the main transport pathways and are mostly void of output synapses, (2) neuritic compartments that contain output synapses, and (3) neuritic compartments that are postsynaptic in nature. In addition we show that mutations of the *kakapo* gene have no obvious effect on the distribution of output synapses in the CNS, whereas neuromuscular synapses are severely reduced. This suggests that synaptogenic mechanisms in the CNS might differ from those at neuromuscular junctions.

Key words: synaptogenesis; development; presynaptic; transplantation; mosaic; kakapo

During development of the nervous system, synapses of the appropriate type have to differentiate and be positioned correctly, so that information flow and processing are orchestrated into functional neuronal circuits. Mechanisms underlying the complex process of synapse formation are poorly understood. To address such mechanisms we chose the embryonic nervous system of *Drosophila melanogaster* because of its defined cellular and developmental context in combination with its genetic amenability and the availability of numerous molecular tools (for review, see Budnik and Gramates, 1999). Like other insects (for review, see Burrows, 1996), *Drosophila* contains identified neurons; i.e., individual neurons can be recognized with respect to the shape and position of their somata and neurites, and many neurons display specific patterns of gene expression (Thomas et al., 1984; Doe and Technau, 1993). From larger insects we know that these identified neurons interact in stereotypic ways with other neurons; i.e., neuronal circuits can be traced back to their individual cellular elements (for review, see Burrows, 1996). So far, studies on synapse formation and function during embryogenesis have been focused mainly on neuromuscular junctions because of their experimental amenability (for review, see Budnik and Gramates, 1999). However, the mechanisms that can be studied at *Drosophila* neuromuscular junctions are limited. First, the postsynaptic cells are muscles; thus neuronal postsynaptic mechanisms cannot be studied (e.g., postsynaptic densities are far more prominent at many synapses in the embryonic CNS than at neuromuscular synapses) (Prokop, 1999). Second, in addition to few neuropeptides and other potential neuromodulators, glutamate seems to be the main transmitter at neuromuscular junctions (NMJs) (Johansen et al., 1989), whereas a larger diversity of neurotransmitters are found to operate in the CNS (for review, see Prokop, 1999). Thus, potential mechanisms specific to nonglutamatergic synapses can be studied only in the CNS.

In the CNS of insects, neurons are monopolar, sending one primary neurite from the cortex (cell body region) into the neuropile (soma-free synaptic area) where they branch and form axons and neuritic arborizations with presynaptic and postsynaptic sites in yet unknown distributions. Ultrastructural analyses of neurons in larger insects have shown that neurites can be specialized (i.e., exclusively presynaptic or postsynaptic), or they can be of mixed nature (for review, see Burrows, 1996). Whether the same organizational principle also applies to the dramatically smaller *Drosophila* neurons, and more specifically, which neurites of various identified interneurons contain presynaptic or postsynaptic sites, has not been investigated so far.

Here we have addressed these shortfalls and show for the first time that output synapses are restricted in a reproducible manner to specific neuritic compartments of individual neurons in the trunk neuropile of *Drosophila* embryos. To this end we applied light-microscopic analyses in combination with mosaic techniques

Received June 27, 2002; revised Sept. 16, 2002; accepted Sept. 18, 2002.

This work was supported by grants from the Deutsche Forschungsgemeinschaft (DFG) (PR605/1 and PR605/2) and the German Israeli Foundation (I 073-203.05/98) to A.P. and by a DFG grant (Bu566/6) to E.B. We express our gratitude to Gerhard M. Technau for advice, helpful discussions, criticism on this manuscript, and provision of lab space and equipment. We are grateful to our colleagues Hugo Bellen, Liqun Luo, Mani Ramaswami, Iain Robinson, John Thomas, and Konrad Zinsmaier and the Bloomington Stock Center for providing fly stocks and antibodies, as named in detail in the text. Furthermore, we thank Matthias Landgraf and Natalia Sánchez-Soriano for constructive and helpful criticism on this manuscript.

Correspondence should be addressed to Andreas Prokop, Institute of Genetics, University of Mainz, J.-J.-Becherweg 32, D-55128 Mainz, Germany. E-mail: prokop@mail.uni-mainz.de.

 0270-6474/02/2210357-11$15.00/0

based on targeted gene expression and a newly developed strategy using established cell transplantation methods. These new insights and techniques are an important prerequisite for future work on synapse formation and structure in the *Drosophila* CNS.

MATERIALS AND METHODS

Fly stocks. Fly strains used in our studies are different mutant alleles of *kakapo* (*kakapo^{sf20}*, *kakapo^{HG25}*, *short stop^{3}*) (vanVactor et al., 1993; Prokop et al., 1998), *tubP-Gal4* (by courtesy of L. Luo) (Lee and Luo, 1999), *elav-Gal4C155* (by courtesy of the Bloomington stock center) (Luo et al., 1994), *Uas-mCD8-green fluorescent protein (GFP)* (second and third chromosome; by courtesy of L. Luo and Bloomington stock center) (Lee and Luo, 1999), *apterous-Gal4* (*ap-Gal4*; by courtesy of John Thomas) (Calleja et al., 1996), *Uas-Synapsin-1^{12}* (this paper), Df(3)Synapsin^{97} (*Syn^{97}*) (Godenschwege et al., 2000), *Uas-Synaptotagmin-hemagglutinin* (*Uas-syt-HA*; by courtesy of I. Robinson) (Robinson et al., 2002), *Synaptotagmin^{AD4}* (*Syt^{AD4}*) (Littleton et al., 1994), and *Uas-neuronal-Synaptobrevin-GFP$^{13.6}$* (*Uas-n-Syb-GFP*; by courtesy of M. Ramaswami) (Ito et al., 1998). To obtain recombinant *kakapo* donor stocks (see Fig. 5*G*), *tubP-Gal4* constructs were jumped from the third to the second chromosome [according to Robertson et al. (1988)]. Recombinations followed standard procedures (Greenspan, 1997).

Generation of Uas-Syn-1^{12} *transgenic flies.* An Xho-PshAI 3.1 kb genomic fragment (containing the exon 1, intron 1, and part of exon 2 of the *Synapsin* gene) of the plasmid rescue vector of the SynP1 (Godenschwege et al., 2000) and a PshAI-XbaI 3.3 kb fragment of the Syn-1 cDNA (containing part of exon 2 and exons 3–13 of the *Synapsin* gene) (Klagges et al., 1996) were cloned into a Xho-XbaI-digested pP(UAST) vector (Brand and Perrimon, 1993). Transformation of *Syn^{97}* mutant flies with the vector containing the *UAS-Syn-1* gene was performed as described elsewhere (Spradling and Rubin, 1982) and resulted in a fly stock carrying a third chromosomal insertion (*UAS-Syn-1^{12},Syn^{97}*).

Immunohistochemistry. Antibodies used in these studies were raised against presynaptic proteins Synapsin (mouse, 1:10) (Klagges et al., 1996), Synaptotagmin (courtesy of H. Bellen) (rabbit, 1:1000) (Littleton et al., 1993), and Cysteine string protein (courtesy of K. Zinsmeier) (Zinsmaier et al., 1990), the transmembrane domain protein CD8 (rat, 1:10; Caltag Laboratories, Burlingame, CA), and the epitope tag hemagglutinin (rat, 1:100; Boehringer Mannheim, Mannheim, Germany).

Dissection, fixation, and staining procedures followed standard protocols (Broadie, 2000). In brief, forceps were used to dissect out CNS from old embryos or larvae. All dissections were performed in external bath solution for electrophysiology (Broadie, 2000). After 30–60 min fixation in 4% paraformaldehyde in 0.05 M phosphate buffer, pH 7–7.2, tissues were washed for 1 hr in PBS with 0.1% Triton X-100 (PBT). Incubation with antibodies was performed in PBT without any blocking reagents, followed by incubation with commercial secondary antibodies (Jackson ImmunoResearch, West Grove, PA; dilution 1:200) coupled to fluorescent dye or horseradish peroxidase. Fluorescent analyses were performed on a Leica confocal microscope true confocal scanner SP2 and Leica confocal software. Horseradish peroxidase was detected via a color reaction in 0.5 mg/ml diaminobenzidine with 0.03% H_2O_2.

Cell transplantations. Cell transplantations were performed as described elsewhere (Prokop and Technau, 1993). In brief, donor and host embryos were of the same stage at ~10 min after the onset of gastrulation. With use of a pulled and ground glass capillary, with an inner diameter of ~10 μm, 10–20 cells were removed from the ventral neurogenic region of the donors at ~0–30% ventrodorsal diameter and at 30% egg length, i.e., in the abdominal region [according to the early gastrula fate map (Prokop and Technau, 1993)]. Single precursors were carefully injected into the same area of the blastoderm of host embryos. Donor embryos were genetically labeled with the cell surface marker CD8, host embryos were mutant for certain synaptic proteins (genotypes described in Results; see Figs. 1*B*, 4*A*). After transplantation, the host embryos were allowed to develop into the final embryonic stage (trachea filled with air). During this time the implanted precursor cells give rise to fully differentiated cell lineages. Most of the development occurred overnight at 25°C, and during the last few hours embryos were shifted to 29°C to enhance Uas-CD8 expression. Fully developed host embryos were dissected and immunostained as described above.

Quantitative analyses. To estimate boutons and output synapses of cell lineages, areas of the lineages were chosen in which synapses were not clustered too densely (see Table 1 legend). With use of Leica confocal software, serial confocal stacks were analyzed section by section, and Synapsin spots of this area were counted on the computer screen. Using Adobe Photoshop software, the circumference of the same area was drawn with the selection tool, and pixel content was determined with the histogram function. To normalize data, the pixel content was divided by the pixel number obtained by measuring and squaring the neuropile width of each respective specimen.

RESULTS

The synaptic area of *Drosophila* is segmentally organized

In the *Drosophila* ventral nerve cord (abdominal and thoracic part of the CNS), segmental ganglia are fused, although segmental units (neuromeres) can still be recognized by distinct landmarks such as the segmental nerves. Each neuromere contains an almost identical set of neuronal cell bodies in typical positions, each of which sends one process into a soma-free zone called neuropile. The neuropile is composed of two connectives (longitudinal tracts) that are connected across the midline in each neuromere by two commissures (transverse tracts) (Fig. 1*B′*). Within the neuropile, neurites of individual neurons are stereotypic and reproducible with respect to their shapes and positions (Udolph et al., 1993; Landgraf et al., 1997; Schrader and Merritt, 2000). All synaptic contacts of the CNS are restricted to neurites in the neuropile as revealed by antibodies against presynaptic proteins such as Synaptotagmin and Synapsin (Fig. 1*A*,*A′*). Their stainings show dense arrangements of little dots in the neuropile representing output synapses (i.e., presynaptic sites or zones). Within this almost homogeneous accumulation of output synapses, reproducible segmental pattern elements like transverse and circular gaps can be seen always in the same positions (Fig. 1*A*,*A′*, *arrows* and *arrowheads*, respectively). Such gaps suggest that certain neurites in reproducible areas of the neuropile might be void of presynaptic sites. We investigated this possibility in larger detail and analyzed distributions of output synapses along individual neurites. To this end we used mosaic analyses based on targeted gene expression and cell transplantations.

Using targeted expression of presynaptic proteins to visualize output synapses

To monitor the localization of presynaptic proteins in small numbers of identified neurons, we first used the Gal4/Uas system of targeted gene expression (Brand and Perrimon, 1993) (Fig. 2*A*). We restricted our analyses to interneurons because they should form output synapses in the CNS (which might not be the case for insect motoneurons) (for review, see Burrows, 1996). To our knowledge, *ap-Gal4* is the only Gal4 driver line with strong and reliable expression in a restricted number of interneurons of late embryos and larvae (two to three interneurons on either side of each neuromere in the ventral nerve cord) (Lundgren et al., 1995) (Fig. 2*B–F‴*). First, we crossed *ap-Gal4* flies to *Uas-CD8-GFP* flies, carrying a construct of the cell surface marker CD8-GFP coupled to the Gal4-responding Uas-sequence. In their offspring (*ap::CD8-GFP* animals) *ap-Gal4* neurons can be visualized with anti-CD8 antibodies (Fig. 2*B*,*E*). Each cell body (Fig. 2, *S*) sends a neurite through the cortex (Fig. 2*C*,*E*,*F*, *open arrows*) that enters the neuropile on its lateral side. From the neuropile entry point, the primary neurites project transversely (Fig. 2, *T*) toward the midline where they join a compact median longitudinal fascicle (Fig. 2, *L*). In the late embryo, small side branches can be seen coming off the transverse primary neurite (Fig 2*B*, *white*

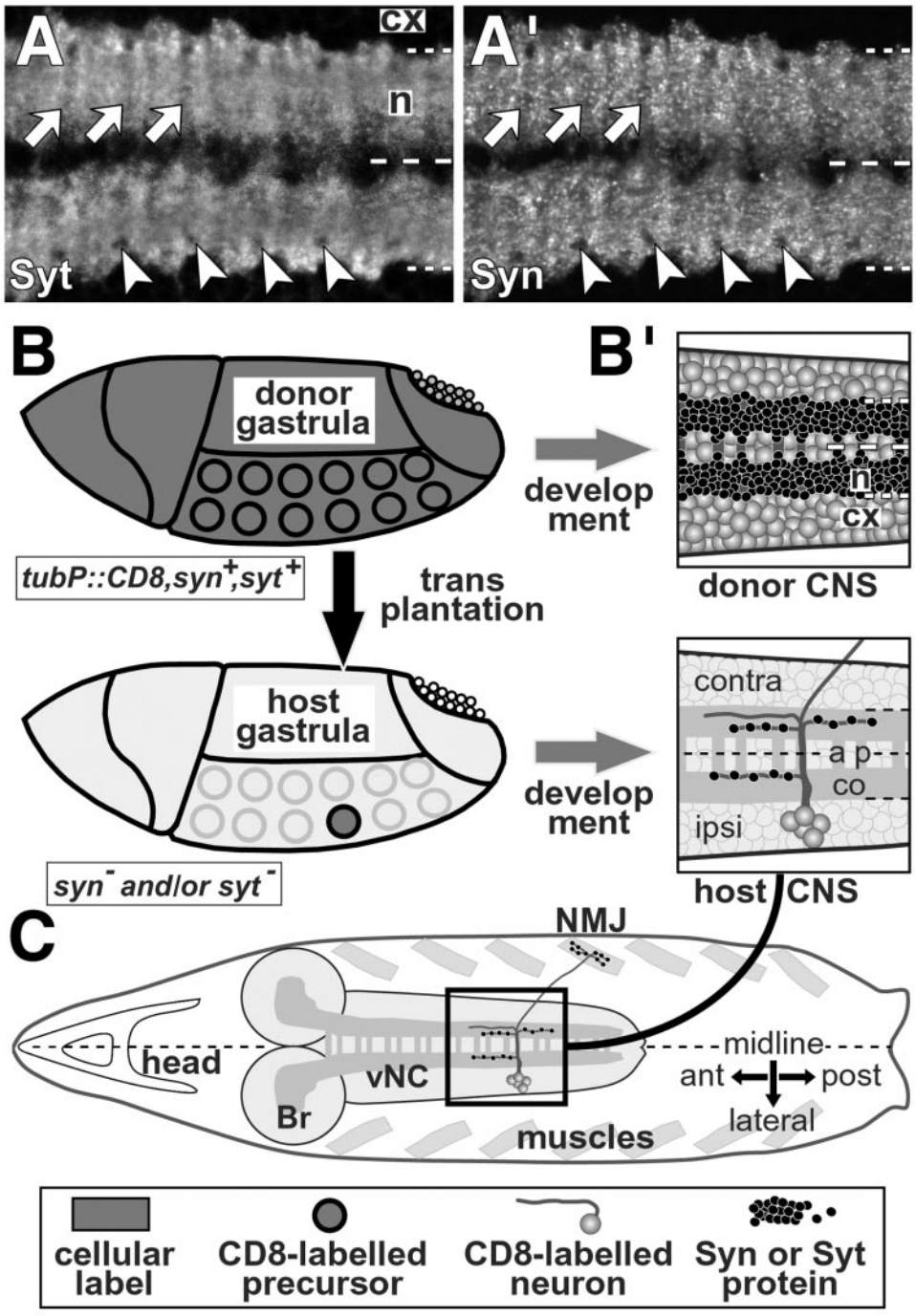

Figure 1. Organization of the embryonic *Drosophila* ventral nerve cord and explanation of the transplantation strategy. *A*, *A′*, Horizontal view (anterior is *left*) of the same confocal plane of a late embryonic ventral nerve cord double labeled for the presynaptic proteins Synaptotagmin (*Syt*) and Synapsin (*Syn*). Both proteins are concentrated in the synaptic (*n*, neuropile; ventral plane shown; *dashed lines* indicate midline and outer limits of neuropile; total width of neuropile, 30–40 μm) but not cell body area (*cx*, cortex) and display the same segmental pattern elements (*arrows*, transverse gaps; *arrowheads*, circular gaps). *B*, Precursor cells (*bold circles*) from the abdominal neurogenic area of donor embryos at the early gastrula stage (genotype: syt^{+}/syt^{+};*tubP-Gal4*,syn^{+}/*Uas-CD8-GFP*,syn^{+}) are transplanted isotopically (*black arrow*) to host embryos of the same age (genotype: Syn^{97}/Syn^{97} or Syt^{AD4}/Syt^{AD4};Syn^{97}/Syn^{97}). *B′*, After development (*gray arrows*) into the late embryonic/early larval stage, the donor CNS displays synaptic proteins (*black dots*) throughout the neuropile (*n*; compare *A*, *A′*) and the surface marker CD8 in all neural cells (*gray shaded circles*; *cx*); the host CNS shows synaptic and surface label only on neurites (*dark gray lines*) and cell bodies of progeny cells derived from the implanted precursor cell. *ipsi*, Ipsilateral (on the side where cell bodies are); *contra*, contralateral (opposite to cell bodies). *Dashed line* represents midline; *gray line* represents neuropile composed of transverse anterior (*a*) and posterior (*p*) commissure and longitudinal connectives (*co*). *C*, Position of images in *B′* within the embryonic/larval body (*ant*, anterior; *Br*, brain; *post*, posterior; *vNC*, ventral nerve cord). Synapses lie in the neuropile (*A*,*A′*, *B′*) but also on muscles at the neuromuscular junction (*NMJ*).

arrow). These side branches are far more elaborate in the late larval nerve cord (Fig. 2*E*, *white arrow*).

To visualize potential presynaptic sites (output synapses) of *ap-Gal4* neurons, we crossed *ap-Gal4* flies with different transgenic fly strains carrying Uas-constructs coding for presynaptic proteins (Fig. 2*A*). To this end, we used *Uas-neuronal-Synaptobrevin-GFP* (visualized for GFP), and *Uas-Syt-HA* (visualized with anti-HA antibodies). In addition, we generated a *Uas-Syn-1*^{12} transgenic fly strain carrying a Uas-construct coding for the presynaptic protein Synapsin (visualized with anti-Synapsin antibodies; intrinsic Synapsin pattern is shown in Figs. 1*A′* and 6*G*,*H*). To restrict Synapsin to *ap-Gal4* neurons, we expressed *Uas-Syn-1* in the absence of intrinsic Synapsin protein using the Syn^{97} mutant allele (*ap-Gal4;Uas-Syn-1*^{12},Syn^{97}). Animals homozygous for Syn^{97} are viable, and preliminary analyses at the light-microscopical, ultrastructural, and physiological levels have failed to reveal any obvious phenotypes (E. Buchner, unpublished results).

Targeted expression of presynaptic proteins suggests differential subcellular distribution of output synapses

When *Uas-n-Syb-GFP*, *Uas-Syt-HA,* or *Uas-Syn-1* is targeted to *ap-Gal4* neurons, immunoreactivity can be detected in the synaptic neuropile (see below). However, staining is also localized to the nonsynaptic cortex, i.e., to Gal4-expressing cell bodies (Fig. 2, *S*) and in punctate patterns along cortical stretches of their

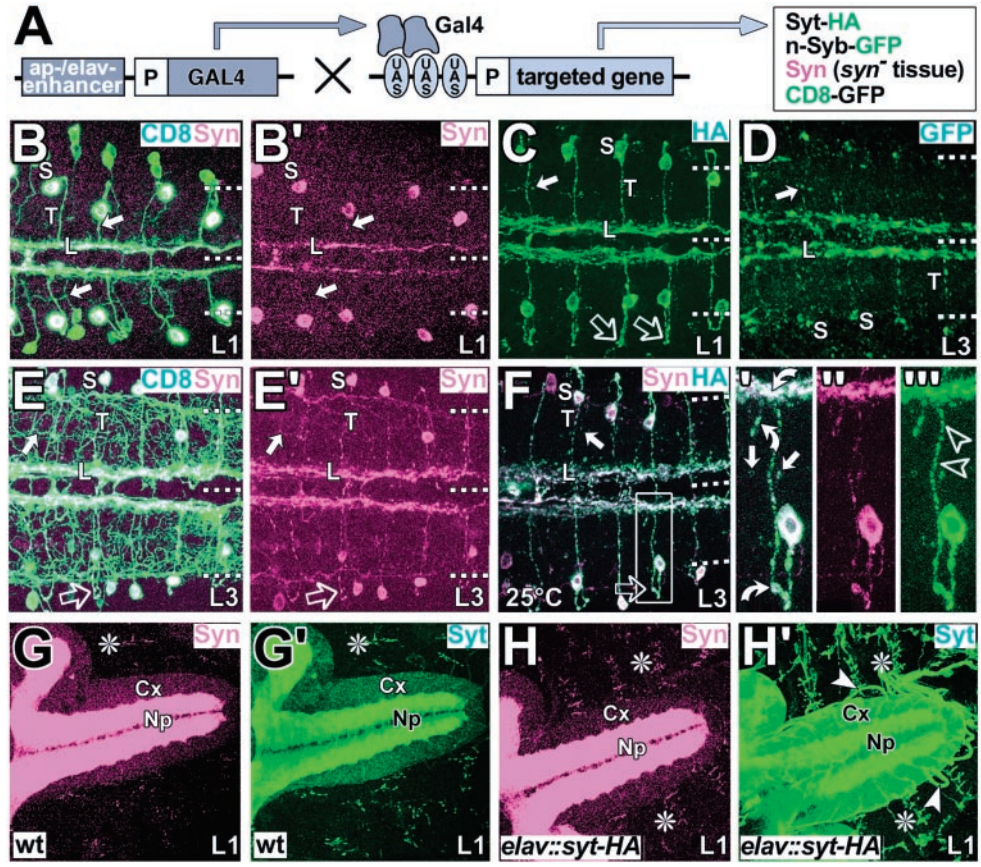

Figure 2. Targeted gene expression was used to visualize synapses in the CNS. *A*, The Gal4/Uas strategy (Brand and Perrimon, 1993): flies carrying the *Gal4* gene (*P*, promoter) coupled to an *apterous*- (*ap*-; cell specific as shown in *B–F‴*) or *elav*-enhancer (pan-neuronal; *H′*) are genetically crossed (*X*) with flies carrying a gene of interest (*targeted gene*) coupled to Uas-promoter sequences; Gal4 protein binds to Uas and induces expression of the targeted gene only in those cells in which *ap*- or *elav*-enhancers are active. Targeted genes used here (*box*) are hemagglutinin-tagged Synaptotagmin (*Syt-HA*), neuronal Synaptobrevin fused to green fluorescence protein (*n-Syb-GFP*), Synapsin (*Syn*; used in Syn^{97} mutant background), and CD8 fused to green fluorescent protein (*CD8-GFP*; cell surface marker). Protein fractions shown in *color* were used for fluorescent immunodetection (indicated at *top right* in *B–H′*; only *G′* and *H′* were stained with anti-Synaptotagmin). *B–F‴*, Ventral nerve cords (anterior is *left*; compare Fig. 1*C*) of larvae right after hatching (*L1*) or late larvae (*L3*) carrying *ap-Gal4* together with different Uas-constructs (*white box* at *top right* indicates the antibodies used as well as Uas-constructs according to *A*). *Dashed lines* indicate midline, neuropile borders, and scale according to Figure 1. The basic morphology (CD8 staining) of *ap*-neurons is the same in L1 (*B*) and L3 (*E*) but more subordinate neurites expand during larval life. *L*, Median longitudinal fascicles; *S*, somata (only in *B* are all 3 *ap-Gal4*-expressing cell bodies per hemi-neuromere shown); *T*, transverse projection; *white arrows*, side branches of primary neurite; *open arrows* in *C*, *E*, and *F*, cortical stretches of primary neurite. *F′–F‴* are magnifications of the *boxed area* in *F*; *F* and *F′* show anti-Syn and anti-HA double labeling; *F″* and *F‴* show only Syn or HA, respectively (*bent arrows*, areas with colocalization of Syn and Syt-HA; *open arrowheads*, localization of only Syt-HA). *G–H′*, Syt is mislocalized in the cortex (*Cx*) and peripheral nerves (*arrowheads*) after strong pan-neuronal overexpression of Syt-HA (*H′* vs *G′*), whereas the distribution of other presynaptic markers is unaffected (*H* vs *G*; *asterisks*, neuromuscular junctions; *Np*, neuropile).

primary neurites (Fig. 2*C*,*E*,*F*, *open arrows*). Thus, after targeted expression, synaptic proteins can be localized to extrasynaptic areas, and this is strongest in *ap::Syt-HA* animals (Fig. 2*C*,*F*). Similar results were obtained when mis-expressing Syt-HA pan-neuronally (*elav::Syt-HA*) (Fig. 2*H′*, *asterisk*). In late *elav::Syt-HA* embryos, significant amounts of targeted Synaptotagmin were found in the cortex and along peripheral nerves (Fig. 2*H′*, *Cx* and *arrowheads*). However, in the same animals, intrinsic Synapsin (Fig. 2*H*) or intrinsic Cysteine string protein (data not shown) showed the usual restricted distribution to the neuropile and neuromuscular junctions (Fig. 2*H*, *Np* and *asterisks*). Thus, the general pattern of intrinsic output synapses seems unaffected by surplus amounts of mis-expressed synaptic proteins. Furthermore, the surplus mis-expressed protein seems to be either localized to transport vesicles (Ahmari et al., 2000) or deposited along extrasynaptic areas of neurites.

Within the neuropile, punctate patterns of targeted proteins reminiscent of output synapses can be seen along *ap-Gal4* processes. In most of these puncta, different targeted proteins seem to colocalize, as demonstrated via coexpression of Syt-HA and Syn-1 in the same Syn^{97} mutant animals (Fig. 2*F′*, *bent arrows*). However, detailed inspection of these animals reveals that Syt-HA, especially, can also occur alone (Fig. 2*F‴*, *open arrowheads*). Therefore, either not all output synapses are equally labeled by all tagged proteins or targeted proteins can localize randomly to ectopic, nonsynaptic sites. However, the overall pattern of targeted proteins shows clear tendencies of preferential localization, which can be obtained with different immunolabeling methods (staining with HRP/DAB/H_2O_2 revealed the same results; data not shown). First, strong and consistent accumulation of all targeted proteins is detectable in the median longitudinal fascicle (Fig. 2, *L*). Second, less consistent stain can be found along the transverse neurites (Fig. 2, *T*). This labeling of the transverse neurites is strong in *ap::Syt-HA* animals (Fig. 2*C*,*F*) but weaker with Syn-1 or n-Syb-GFP. For Syn-1 it is even weaker at 18°C (where Gal4-activity is lower; data not shown). These variabilities suggest that the dotted stain in transverse projections might not represent true output synapses but surplus extrasynaptic protein, similar to stain found in cortical areas (see above and Discussion). Third, the only neurites that are consistently free of any of the targeted proteins (except for very occasional dots) are the side branches coming off the transverse primary neurite, suggesting that these side branches might be preferentially postsynaptic (Fig. 2, *white arrows*).

Taken together, our stainings suggest that output synapses seem to be localized preferentially to the median longitudinal fascicles formed by *ap-Gal4* neurons (see Discussion). However, our findings just reveal tendencies that are obscured by potentially extrasynaptic localization of targeted proteins in *ap-Gal4* neurons.

Using transplantation-based mosaic analysis for the visualization of output synapses in the CNS of *Drosophila*

Caveats regarding the Gal4/Uas approach are the limited number of suitable Gal4-lines and the artificial expression levels of targeted proteins resulting in restricted reliability for the identification of true output synapses. To overcome these problems, we established a new way of mosaic analysis that allows the visualization of intrinsically regulated presynaptic proteins in all neural cell lineages.

This technique is based on cell transplantation of single precursor cells (Prokop and Technau, 1993) (Fig. 1*B*,*B′*): a single cell from the neuroectoderm is transplanted from a labeled donor into an unlabeled host embryo at the early gastrula stage. There are 35 different neural precursors in each presumptive hemineuromere of the ventral nerve cord of *Drosophila* that can develop from these transplanted cells. All of their lineages have been shown to be reproducible, and detailed descriptions have been published (Bossing and Technau, 1994; Bossing et al., 1996; Schmidt et al., 1997, 1999). To visualize presynaptic sites, we use wild-type donor embryos carrying one copy of a Gal4 construct under the control of the ubiquitous *tubulinP*-enhancer and one copy of the *Uas-CD8-GFP* construct. Cells from these donors are transplanted into hosts that are homozygous for the Syn^{97} deletion (Fig. 1*B*). At the end of embryogenesis, their CNSs are removed, fixed, and stained with anti-CD8 and anti-Synapsin antibodies (Fig. 1*B′*). Because only the transplantation-derived cells express the surface marker CD8, their projections can be visualized. Additionally, they are the only cells expressing the presynaptic protein Synapsin, which can be seen exclusively along CD8-labeled processes. Because Synapsin expression in these cells is based on the natural intrinsic control, its spot-like staining should represent true output synapses of these neurons.

Our analyses were performed at the end of embryogenesis, thus later than previous studies on identified embryonic neuronal lineages that were restricted to early and mid stage 17, i.e., stages in which cuticle is not yet fully developed (Schmidt et al., 1997, 1999). At the late embryonic stage, projections have grown further, and additional neurites have developed (Fig. 3). Furthermore, because of condensation of the nerve cord, cell bodies have often changed their position, the space between the neuropiles of both body halves is severely reduced, and the outlines of anterior and posterior commissures are less obvious. Nevertheless, a certain number of cell lineages could be identified with respect to published data for younger embryos (Table 1). Detailed descriptions and criteria used for their identification will be published elsewhere (but see examples in Fig. 3). Here we will focus on features relevant to the addressed topic.

Synapsin staining and Synaptotagmin staining of cell lineages are specific and reproducible

Strikingly, any cell lineages that were obtained more than once showed a reproducible distribution of Synapsin (Figs. 4, 5). Minor variations were observed, and these might reflect either a degree of inherent variability of these cells or limitations of the method. Such variations never obscured the clearly conserved overall pattern of lineage-specific Synapsin distribution. We wondered whether Synapsin might reflect an incomplete pattern of synapse distribution. To test this possibility we made use of the presynaptic protein Synaptotagmin, which is essential for synapse function and for which antibodies and protein null mutations are available (Littleton et al., 1993; Südhof and Scheller, 2001). Using Syt^{AD4};Syn^{97} double-mutant embryos as hosts, we transplanted precursor cells from *tubP::CD8* donors and obtained some cell lineages double labeled with anti-Synapsin and anti-Synaptotagmin. In these cell lineages, both proteins were generally colocalizing (Fig. 4*I*,*J*, *white arrows* and *arrowheads*). In some cases we could see rare spots labeled with Synaptotagmin alone; however, they intermingled with double-stained sites and therefore did not alter the principal pattern of potential output synapses (Fig. 4*J*, *white Vs*). Some specimens were stained with only anti-Synaptotagmin and anti-CD8 antibodies. Resulting cases of identifiable lineages revealed a distribution of presynaptic spots that matched very well with images obtained from other examples of the same lineage labeled with anti-Synapsin and anti-CD8 (Fig. 4, *G* vs *H*).

Thus, our transplantation-based mosaic analyses with two different presynaptic proteins reveal the same reproducible distribution of presynaptic sites within neuronal cell lineages of *Drosophila* embryos and strongly suggest that output synapses can be reliably visualized with this technique.

Output synapses of cell lineages are restricted to specific neuropile areas

The distribution of output synapses within cell lineages can be restricted within the dorsoventral, ipsilateral–contralateral, anteroposterior, or mediolateral axis (Table 1). For example, lineages containing ventral unpaired median neurons (VUMs) (Fig. 4*B*,*B′*) contain two to six cells, which are located at the ventral midline of the nerve cord. Half of the VUM neurons are usually bifurcating motoneurons, and the other half are bifurcating interneurons (Bossing and Technau, 1994). The neurites of the VUM neurons can be seen from dorsal to median levels within the neuropile. Frontal presentations of such lineages demonstrate clearly that only projections in the more ventral area bear output synapses (Fig. 4*B′ii*, *white arrowheads*), whereas dorsal neurites are free of Synapsin stain (Fig. 4*B′ii*, *open arrowheads*). A very similar result was observed for a further median cell lineage derived from the median neuroblast (MNB) (Bossing and Technau, 1994) (Figs. 4*A*, 5*C*). In the NB5-2 lineage, anterior contralateral projections bear output synapses in the dorsal but not ventral plane of the neuropile (Fig. 4*G*,*H*, *open* versus *white arrowheads* on *left side* in *i* vs *ii*, respectively). Similarly, the cell lineages derived from the precursors NB2-1, NB3-1, and NB5-3 show a dorsoventral-specific distribution of presynaptic sites within their neurites (data not shown).

Examples for ipsilateral–contralateral-specific distribution of output synapses are the cell lineages of NB1-1, NB3-2, NB5-3, and NB7-1. All lineages have neurites on both sides of the nerve cord. In the case of NB7-1, only contralateral projections bear output synapses (Fig. 4*F*,*F′*, *white arrows* and *arrowheads*). The same is true for NB3-2 and NB5-3, whereas NB1-1 restricts output synapses to ipsilateral projections (data not shown).

Anteroposterior-specific distribution of output synapses can be found in the lineages of NB6-1 and NB6-2 (Figs. 4*D–E′*, 5*B*). The NB6-1 lineage has neurites on the ipsilateral and contralateral side, which are directed anteriorly and posteriorly. Although on the contralateral side projections to posterior and anterior show Synapsin staining, anterior projections on the ipsilateral side are free of output synapses (Fig. 4*D*,*D′*, *open arrowheads*). An even more striking example of specific anterior–posterior distribution is the cell lineage of NB6-2. Its neurons have ipsilateral and contralateral neurites, and output synapses can be seen on both sides. Contralaterally, most projections turn posterior, and there

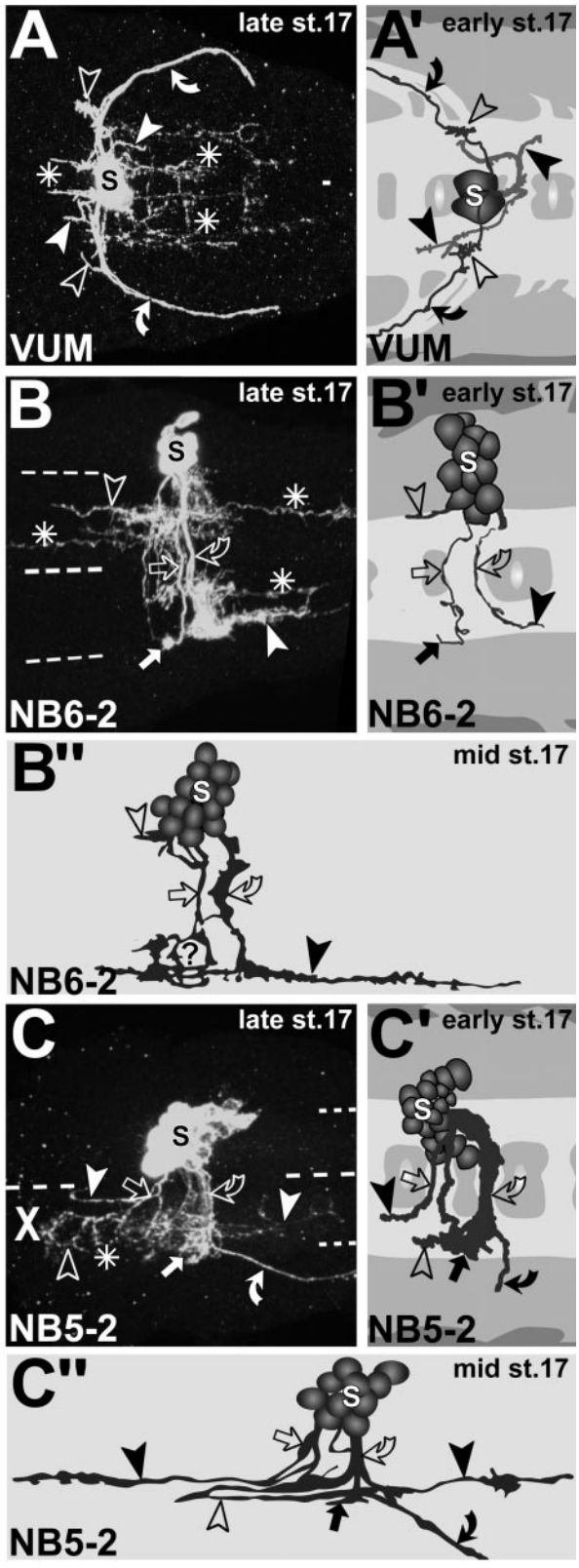

Figure 3. Examples of neural lineages at early, mid, and late stage 17. *A–C*, Three examples of anti-CD8-stained cell lineages of late stage 17 embryos obtained from our transplantation experiments (lineage name indicated at *bottom left*; stage indicated at *top right*). Pictures with primed numbers show examples of the same lineage at earlier stages according to previous publications [pictures were taken and modified from the following publications: *A′*, Bossing and Technau (1994); *B′*, *C′*, Bossing et al. (1996); *B″*, *C″*, Schmid et al. (1999)]. *Symbols* indicate the potentially same structures of each lineage at different stages (exception: *X*, physical damage of specimen causing short appearance of projections; *?*, area difficult to assign to later stage). Lineages at late stage 17 have increased and refined their neurite patterns (examples are indicated by *asterisks*). Clones were identified using the following criteria. VUM lineages lie medial and have bifurcating motoneuronal (*bent arrows*) and interneuronal (*arrowheads*) projections and can only be mistaken for the MNB lineage. However, VUM neurons are located more ventrally (data not shown), contain in most cases only two neurons (*S*), and half of the cells represent motoneurons in cases of four- or six-cell VUM clones (Bossing and Technau, 1994). NB5-2 lineages carry a contralateral efferent projection (*bent arrow*), which is true only for NB5-2, NB2-4, and NB3-1. However, they can be distinguished because NB2-4 has fewer somata that are located more laterally, and NB3-1 has fewer cells, including some characteristic motoneuronal cell bodies in the mediodorsal position (Bossing et al., 1996; Schmid et al., 1999). NB6-2 has no efferent projections and more than one axonal fascicle crossing the midline (*open straight* and *bent arrows*). These criteria would also fit NB4-1 and NB1-2; however, somata of NB4-1 are located more median, and NB1-2 has a characteristic isolated TB neuron (Bossing et al., 1996; Schmid et al., 1999).

is a sharp line behind which output synapses can be found (Fig. 4*E*,*E′*, *asterisks*) (less obvious in Fig. 5*B* because of age of specimen as explained in legend). Except for a single focal accumulation of output synapses (Fig. 4*E*,*E′*, *white arrow*), the anteriorly located contralateral neurites are devoid of output synapses.

The neural lineages of NB3-1 (data not shown), NB6-2, and NB2-1 show a mediolateral-specific distribution of output synapses. In NB6-2, an ipsilateral neurite projecting anterior along a intermediate longitudinal tract is free of Synapsin spots (Figs. 4*E*, 5*B*, *open arrowhead*; less visible in Fig. 4*E′*), whereas the more median ipsilateral anterior projections show output synapses. Vice versa, on the contralateral side, laterally located anterior projections show presynaptic staining, whereas more medially located projections do not (Figs. 4*E*,*E′*, Fig. 5*B*, *open* vs *white arrow* on the *left*). Neurons of the NB2-1 lineage project to the contralateral side where they form medial and lateral arborizations. Only the laterally located projections show presynaptic spots (Fig. 4*C*,*C′*, *white arrow* vs *open arrowhead*).

Output synapses are reproducibly restricted to compartments of neurites

Taken together, our analyses demonstrate that some neuronal processes harbor output synapses, whereas others do not. Furthermore, our lineages demonstrate that those neurites that have output synapses have them restricted mostly to reproducible neuritic compartments. For example, in the cell lineages of neuroblasts 2-1, 3-1, 3-2, 5-2, 5-3, 6-1, 6-2, and 7-1, neurites enter the neuropile ipsilaterally and cross the midline. Contralaterally the neurites reach into defined areas of the neuropile and form branches. Often output synapses can be seen only on these contralateral branches, whereas the transverse primary neurites are void of stain (Figs. 4, 5, *open straight* and *bent arrows*). This phenomenon is most striking for the lineages of neuroblasts 2-1 and 6-2, because in these lineages more or less isolated neurites can be seen that bear accumulations of output synapses only at their very tips (Figs. 4*C*,*C′*,*E*,*E′*, 5*B*, *white arrows*). Other examples become very obvious when we scroll through the different focal planes of our preparations, but they are mostly obscured when pictures are compressed into one layer (data not shown). In those examples mentioned for NB2-1 and 6-2, presynaptic arbors are restricted to a small area (Figs. 4*C*,*C′*,*E*,*E′*, 5*B*, *white arrows*), indicating that these cells represent local interneurons. In many

Table 1. Summary of wild-type lineages

Lineage description			Output synapse distribution					Synapse count		Presynaptic arbor area	
Name	*n* (wt)	Figure	DV	CI	AP	ML	Compart	wt	*kak*	wt	*kak*
VUM	8	4*B*, *B*	X				−	−	−		
MNB	2	4*A*, 4*F*	X				−	33 and 64	37	0.4 and 0.46	0.51
NB1-1	2	−		X			−	13 and 26	16	0.1 and 0.06	0.1
NB2-1	2	4*C*, *C′*	X			X	+	−	−		
NB3-1	2	−	X			X	+	−	−		
NB3-2	10	−		X			+	39 to 81 57.3 ± 13.72	52	0.1 to 0.21 0.14 ± 0.033	0.19
NB5-2	12	4*G*, *H*, 5D	X	X			+	24–56 40.7 ± 10.35	37	0.16 to 0.33 0.25 ± 0.063	0.21
NB5-3	3	−	X	X			+	−	−		
NB6-1	4	4*D*, *D′*			X		+	−	−		
NB6-2	8	4*E*, *E′*, 5*E*			X	X	+	46–80 64 ± 12,86	(40?) (Damage)	−	(?) (Damage)
NB7-1	2	4*F*, *F′*		X			+	−	−		

Lineage description: Name, name of neural precursor that the lineage is assigned to; *n* (wt), number of wild-type lineages obtained; Figure, reference to images shown in this paper. Output synapse distribution: output synapses show specific dorsoventral (DV), contralateral–ipsilateral (CI), anteroposterior (AP), or mediolateral (ML) distribution, or reveal (+)/lack (−) obvious compartmentalized distribution in individual neurites (Compart). Synapse count: Counts of individual Synapsin spots of wild-type (wt) or *kakapo* (*kak*) mutant cell lineages (in cases of $n > 2$: lowest to highest number; mean ± SD; Damage, synapse number in the *kakapo* mutant NB6-2 lineage might be low because of distortion of the preparation; see Fig. 5*E*). Counts were performed on serial confocal sections and restricted to defined areas of lineages in which spots could be reliably resolved. Defined areas were as follows: MNB, total; NB1-1, all posterior ipsilateral spots; NB3-2, total; NB5-2, all contralateral spots anterior of characteristic transverse projection (indicated by *arrow* in Figs. 4, *G* and *H*, and 5, *A* and *D*). Presynaptic arbor area, Areas covered by the counted Synapsin spots; values represent measured presynaptic area divided by the square of the neuropile width of each respective neuropile.

other cases the presynaptic arbors coming off transverse neurites seem to lie predominantly in longitudinal tracts and often extend across neuromere borders (potential intersegmental interneurons) (Figs. 4, 5, *white arrowheads*).

Our lineage analyses show clearly that output synapses are often restricted to reproducible compartments on individual neurites. Preferentially primary transverse neurites are void of output synapses. Our transplantation experiments are in agreement with our observations from the experiments with *ap-Gal4* and encourage use of both methods for future investigations of mechanisms underlying synapse formation and localization in the *Drosophila* CNS.

Mechanisms underlying formation of output synapses in the CNS and at neuromuscular junctions might differ

Having learned about basic principles of synapse distribution in central neurons, we have begun to apply this knowledge and our transplantation strategy for the genetic analysis of synaptogenesis in the CNS. Thus, we ask whether mutations affecting the development of NMJs (Fig. 1*C*) might also interfere with synaptogenesis in the CNS. Mutations of the cytoskeletal interacting factor Kakapo (also called "Short stop") show a severe reduction of output synapses at embryonic motor terminals of *Drosophila* (Prokop et al., 1998) (Fig. 6, *J* vs *H*). Furthermore, *kakapo* mutations show defects in the CNS (reduced neurites and failure to compartmentalize the transmembrane protein Fasciclin 2) (Prokop et al., 1998), but these CNS phenotypes have not been studied at the synaptic level. To perform such analyses, we generated recombinant fly stocks that allow labeling and identification of *kakapo*-mutant cell lineages (*tubP-Gal4,kak*$^{Df(2R)MK1}$/*Uas-CD8-GFP,kak*^{sf20}) (Fig. 5*G*). Using these embryos as donors for transplantations and *kak*$^{+}$*;Syn*^{97} embryos as recipients, we obtained cell lineages of NB5-2 (Fig. 5*D*), NB6-2 (Fig. 5*E*), MNB (Fig. 5*F*), NB1-1 (data not shown), and NB3-2 (data not shown). For reasons yet unknown, most examples of mutant lineages (except NB6-2) displayed an extremely weak and discontinuous CD8 staining so that the precise shape and extent of neurites could not be analyzed in detail. However, all of these lineages showed strong Synapsin staining, making it easier to interpret the location of the presynaptic projections. Output synapses seemed clearly present as revealed by strong dots of Synapsin staining, although they appeared slightly blurred and extended compared with wild type, and occasionally Synapsin seemed to aggregate into larger spots than usual. However, compartmentalization of output synapses seemed normal with respect to the criteria described before for the respective wild-type lineages. More surprisingly, the amount of output synapses was not different from wild-type lineages when single Synapsin spots were counted in our specimens nor was the area over which the synaptic spots were distributed (Table 1) (for one special exception, see Fig. 5*E*, *X*). In contrast, motoneuronal terminals and the number of neuromuscular output synapses in these donor embryos were strongly reduced, in agreement with previous descriptions (Fig. 6, *J* vs *H*, *arrows*) (Prokop et al., 1998). One explanation for the mild phenotypes in the CNS might be that the analysis of single mutant cell lineages might be rescued via some non-cell-autonomous contribution of the surrounding wild-typic host tissue. However, our analyses of *kakapo*^{sf20}/*kakapo*$^{Df(2R)MK1}$ mutant CNS likewise showed a rather normal amount of Synapsin staining and even maintained segmentally repeated pattern elements described for the wild-type neuropile earlier in the text (Fig. 6, *I* vs *G*). Two further *kakapo*-mutant alleles (*short stop*^{3}) (Fig. 6*M*,*N*) and *kakapo*^{HG25} (data not shown) similarly showed affected NMJs but normal amounts of synaptic staining in the neuropile, regardless of the presynaptic marker that we used for our analyses.

Hence, *kakapo*-mutant embryos show strong reduction of output synapses at the NMJ but surprisingly little effects on the distribution and amount of presynaptic stain in the CNS. This suggests that molecular mechanisms of synaptogenesis might differ to a certain degree in the CNS and at motor terminals, a

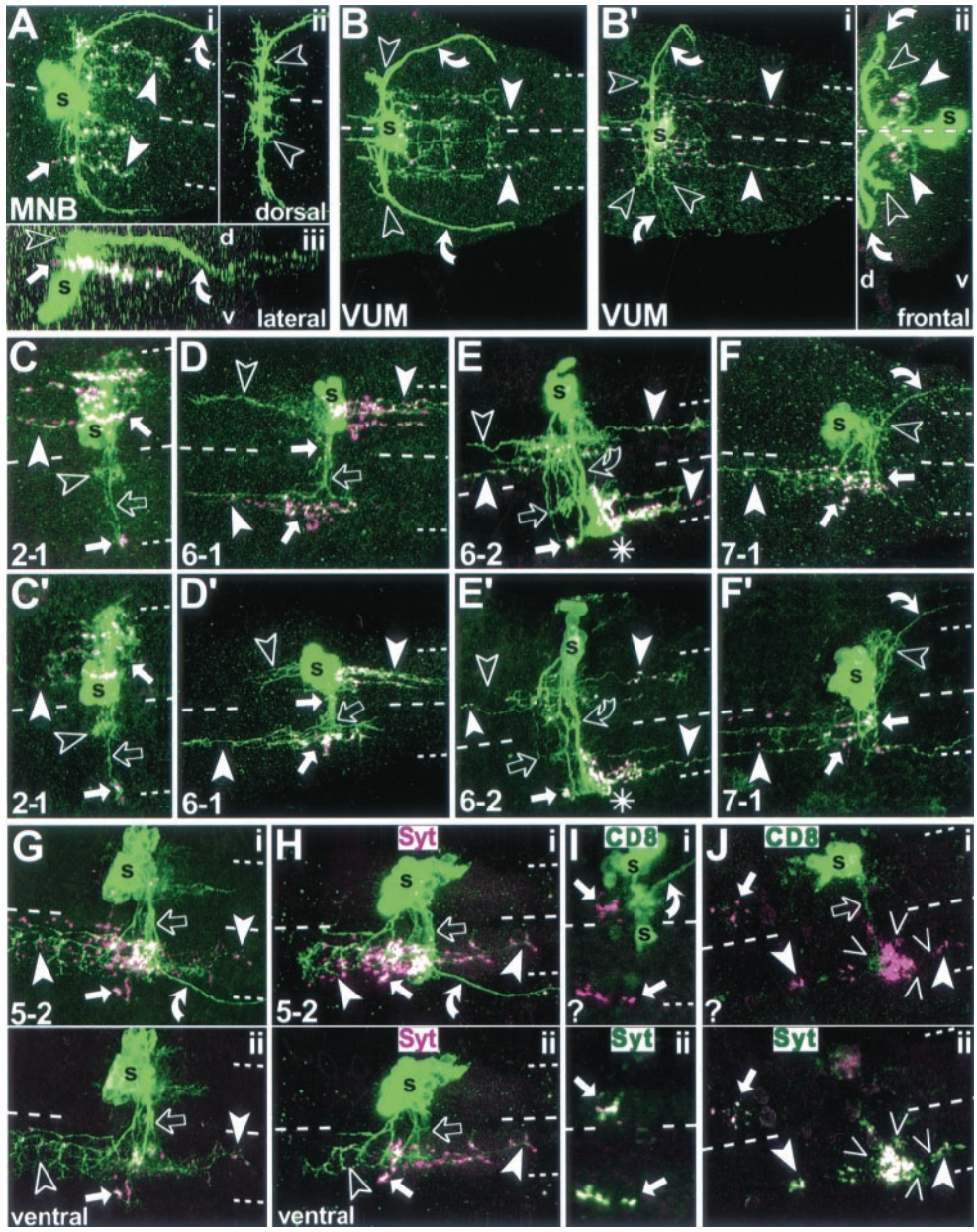

Figure 4. Examples of cell lineages obtained from transplantations of neural precursors. Horizontal (except *Aiii* and *B′ii*) confocal images (anterior is *left*) of transplantation-derived cell lineages in the ventral nerve cord of late embryos (compare Fig. 1*B′*,*C*) labeled with anti-CD8 (*green*; all images except *Iii*, *Jii*) and anti-Synapsin (*magenta*; all images except *H*) or anti-Synaptotagmin (*magenta* in *H* and *green* in *Iii*, *Jii*). The *i*-labeled images show different aspects of the same specimen: *Aii*, only dorsal plane; *Aiii*, image stack turned into lateral view (*d*, dorsal; *v*, ventral); *B′ii*, turned into frontal view; *Gii* and *Hii*, only ventral plane). Primed and unprimed versions of the same letter represent independent examples of the same cell lineage (name indicated at *bottom left*, in *I* and *J* not identified; *symbols* indicate same structural features). General symbols used: *S*, somata (cell bodies); *bent white arrows*, efferent projections; *white symbols* (*arrows*, *arrowheads*, and *asterisks*), characteristic arrangements of presynaptic stain; *open symbols* (*arrows*, *arrowheads*, and *bent arrows*), characteristic neurites lacking output synapses; *triangles* (in *J*), synaptic spots with only Syt label. Occasional Synapsin stain in cell bodies is an artifact and does not represent true localization. Some longitudinal projections in *F′* are hard to see, and cell bodies in *F′* are shifted more toward midline. *Dashed lines* indicate midline, neuropile borders, and scale according to Fig. 1.

possibility that needs to be considered for future work. Furthermore, our experiments with *kakapo*-mutant embryos show that the transplantation technique can be combined with genetic approaches and represents an important method for future analyses of mechanisms underlying synapse formation in the CNS.

DISCUSSION

Output synapses are compartmentalized on neurites of embryonic *Drosophila* neurons

Here we show for the first time the restricted localization of output synapses to specific neuritic compartments in the CNS of *Drosophila* and that they are distributed in reproducible patterns. Our results suggest the existence of at least three different types of neurites or neuritic compartments. First, a fraction of neurites clearly harbors output synapses that have the tendency either to be arranged into longitudinal tracts (Figs. 4, 5, *white arrowheads*) or to form local arborizations (Figs. 4, 5, *white arrows*).

Second, especially transversely oriented (primary) neurites leading toward output areas are usually void of Synapsin in our transplantation-derived specimens and might represent transport highways. This might explain the random dots of staining when synaptic proteins are targeted to *apterous-Gal4* (Fig. 2, *T*), which might be attributable to the fact that excess amounts of targeted protein are traveling in these transverse neurites (Ahmari et al., 2000) or get deposited on their way. We are not aware of data showing that vertebrate neurons might compartmentalize their output synapses along their axons and nondendritic neurites (Peters et al., 1991), although one would perhaps expect that they do. For example, parallel fibers in the cerebellum might first project through the Purkinje cell layer but not form output synapses before they reach the molecular layer. On the other hand, cultured hippocampal neurons show no obvious compartmentalization of output synapses in nondendritic processes (Rao et al., 2000), but this might not reflect the situation within the intact brain tissue.

Third, our *apterous-Gal4* experiments revealed that branches

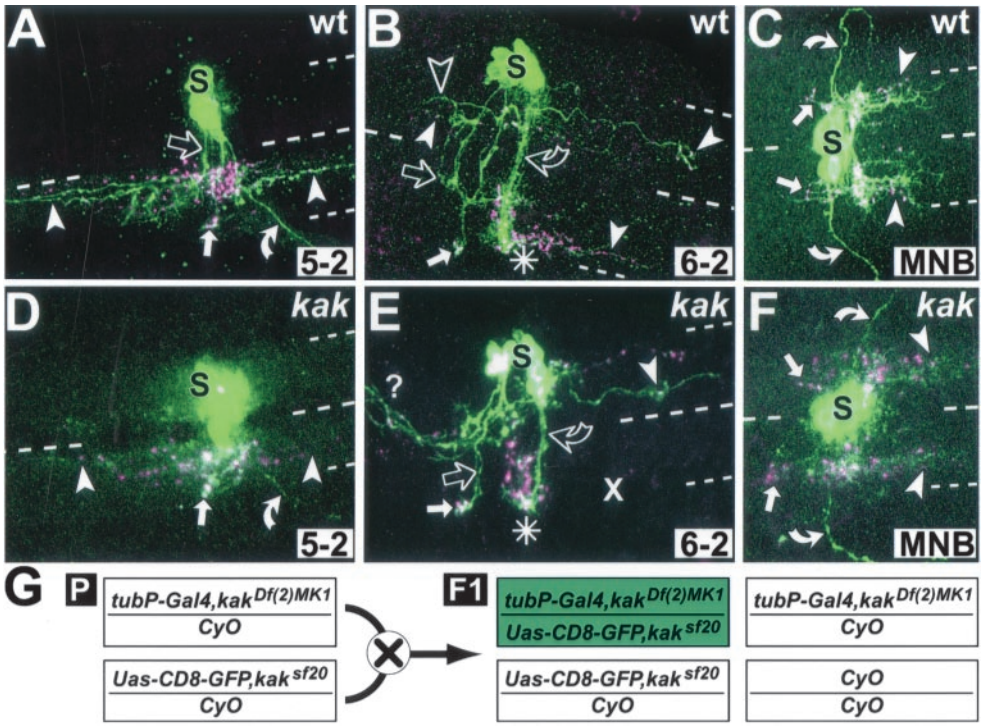

Figure 5. Clonal analysis of *kakapo*-mutant neurons. *A–F*, Examples of same lineages (name indicated at *bottom right*) in wild-type (*A–C*) and *kakapo*-mutant version (*D–F*). Projections in *kakapo*-mutant lineages are poorly visible for reasons unknown. Example in *E* is damaged in the anterior (*?*) and posterior area (*X*). Specimens in *B* and *E* are slightly younger (compare Fig. 4*E*,*E′*) as revealed by location and density of synaptic spots and less condensed arrangement of transverse projections (*bent open arrow*). For further explanations of symbols and scale, see legends of Figures 1 and 4. For reasons of clarity, the Synapsin pattern of the lineages in *A–F* is shown also in *black* and *white* in Figure 6. *G*, Donor embryos used in transplantation experiments (according to Fig. 1*B*) were the progeny (*F1*) derived from crosses (*X*) of parental flies (*P*) carrying different *kakapo* (*kak*) alleles. Because *kak* was recombined onto one chromosome with either *tubP-Gal4* or *Uas-CD8-GFP*, respectively (kept over CyO balancer chromosomes), the only F1 embryos expressing CD8 pan-neuronally (*green box*) are *kakapo*-mutant according to Mendelian rules.

coming off the primary neurite on its way through the neuropile were basically void of the mis-expressed presynaptic proteins. Also, unstained neurites could be found in the transplantation-derived specimens (Figs. 4, 5, *open arrowheads*). Such neurites might represent true postsynaptic structures, as found similarly for neurons in larger insects (Killmann et al., 1999) (for review, see Burrows, 1996). Indeed, our present investigations show that certain neurites of *Drosophila* neurons share several features with postsynaptic vertebrate dendrites (unpublished observations).

So far, statements about compartmentalization of neurites could be made only for repetitively organized neural tissues of the CNS. For example, the distribution of synaptic markers in the repetitively organized optic lobes of flies reveals that primary neurites have stretches of nonsynaptic surfaces because they project through synapse-free areas among lamina, medulla, and lobula/lobula plate (Hiesinger et al., 1999; Meinertzhagen and Sorra, 2001). Also, output synapses on the efferent projections of motoneurons are clearly restricted to the neuromuscular terminal (Fig. 6*H*). The situation was unclear for more diffuse regions like the neuropile of the ventral nerve cord, and our studies are the first to uncover the synaptic distribution at the level of individual projections.

Two different strategies to visualize synapses within individual neurites

To gain insight into the subcellular organization of neurons in the *Drosophila* CNS, we used light-microscopic analyses of genetic mosaics, either obtained from transplantations or with the Gal4/Uas-system. For our lineage analyses we modified existing techniques (Prokop and Technau, 1993) with respect to the genotypes of host and donor embryos and the stage of analysis (Fig. 1). This allows the visualization of the true intrinsic expression and localization profile of presynaptic proteins such as Synapsin and Synaptotagmin. This cannot be achieved with genetic methods of clonal analysis that require heterozygous backgrounds (for example, the mosaic analysis with a repressible cell marker technique) (Lee and Luo, 1999). In contrast, our approach requires a homozygous mutant condition in which the antigen is absent in all but the implanted cells. Our transplantation-based strategy can be used in different ways. First, as demonstrated for *kakapo*, either donor or host embryos can carry mutant alleles of potential synaptogenic genes, allowing tests for cell-autonomous versus signal-dependent requirements of these genes. Second, donor or host embryos can mis-express genes of interest to test their function in greater cellular detail. Third, the stage of analysis is not restricted to the embryo (Prokop and Technau, 1991). Fourth, our method has the potential to be used for the study of the subcellular localization or cell specificity of any other neural gene, provided that good antibodies are available, and mutant alleles, which eliminate the antigen in host embryos (but do not cause severe phenotypes). A disadvantage of the technique lies in the randomized choice of the precursors, which are transplanted. The choice can be narrowed down only within the dorsoventral axis of the neuroectoderm (Prokop and Technau, 1993), thus restricting the number of different lineages that will be obtained (e.g., most of our experiments were restricted to the ventromedian half of the neuroectoderm). However, once lineages are identified and described, they can be used as templates for further studies, as we have successfully demonstrated for the analysis of *kakapo*-mutant cell lineages.

The Gal4/Uas-based strategy (Brand and Perrimon, 1993) of synapse visualization uses targeted expression of presynaptic proteins and their detection via epitope tags (n-Syb-GFP, Syt-HA) or via genetic removal of the respective intrinsic protein from the whole nervous system (*Uas-Syn-1*^{12} in *Syn*^{97} background) (Fig. 2). The strength of this technique is the ease of its application and the amount of data that can be produced in a short period of time (Ito et al., 1998; Blagburn et al., 1999; Ahmari et al., 2000; Vosshall et al., 2000). The disadvantage of mosaic analyses via targeted expression of synaptic proteins lies in the low number of available Gal4 lines with restricted neuronal expression patterns in late embryos

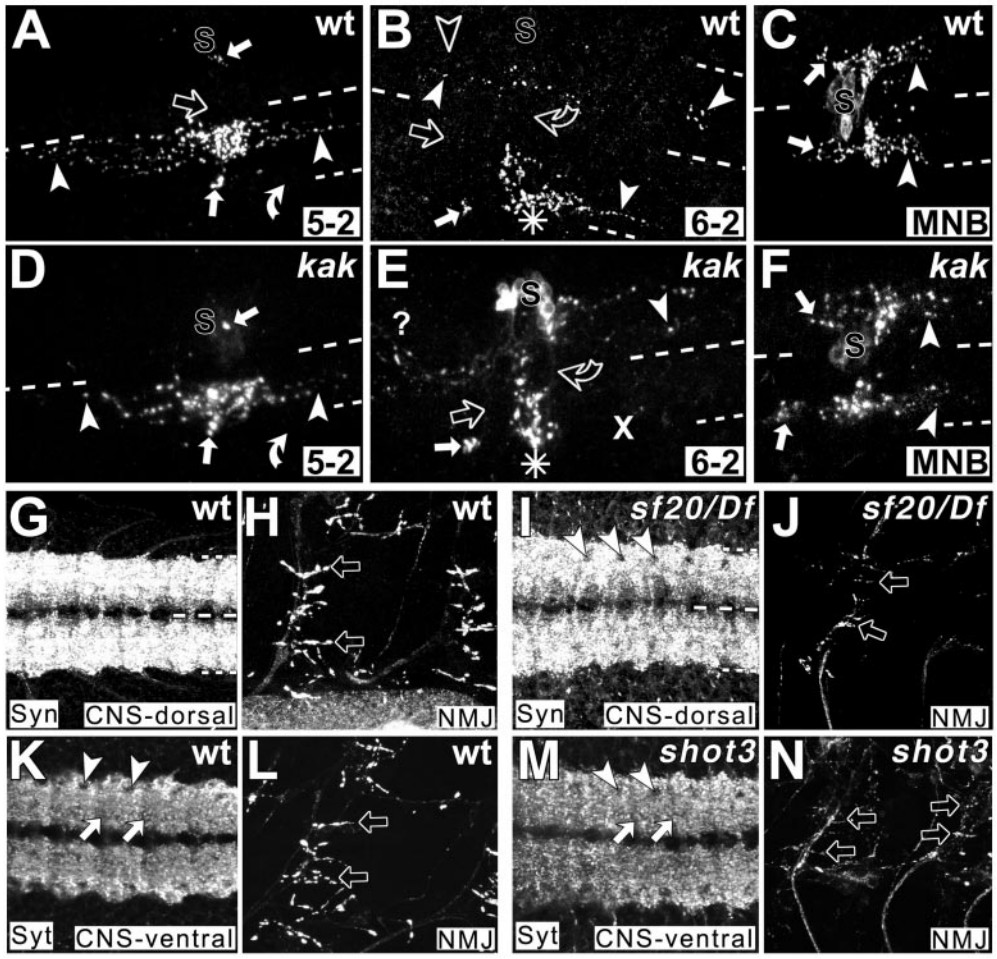

Figure 6. Pattern of central and neuromuscular output synapses in *kakapo*-mutant embryos. *A–F*, Images of Figure 5*A–F* shown in the absence of the partially disturbing green label of neurites. Arrangements of panels and symbols is identical to those shown in Figure 5*A–F*. *White stain* represents Synapsin stain throughout. *G–J*, Synapsin staining of the CNS (dorsal neuropile area) and neuromuscular junctions (*NMJ*; *white arrows* in *H*, *J*) of control (*wt*; *G*, *H*) and $kakapo^{sf20}/kakapo^{DfMK1}$-mutant donor embryos (*sf20/Df*; *I*, *J*). *K–N*, The same phenotypes are revealed by Synaptotagmin staining of the CNS (ventral neuropile area) and NMJs (*open arrows*) in control embryos *(wt*; *K, L)* and *short stop*^{3} (*shot3*; another allele of *kakapo*; *M*, *N*). With either marker (*Syn* or *Syt*) and in both mutant alleles, pattern elements (*white arrows*, transverse gaps; *white arrowheads*, round gaps) occur normally in the ventral neuropile (here only shown for *shot3*; see *M* vs *K*), and additional round gaps occur in the dorsal neuropile (here only shown for *sf20/Df*; *white arrows* in *I* vs *G*).

or larvae. This limits the experimental possibilities, and results can hardly be generalized. Furthermore, experimenters will have to take into consideration the fact that extrasynaptic staining might occur, especially when constitutively active Gal4 drivers cause overproduction of the protein (Fig. 2). In contrast, intrinsically regulated synaptic proteins are restricted to the neuropile and NMJs in mature embryos (Figs. 1*A*,*A′*, 6*G*,*H*). Nevertheless, our analyses in the ventral nerve cord of *apterous-Gal4* embryos and larvae suggest that preferential output areas of Gal4-expressing neurons can be visualized. In agreement with the model derived from our transplantation studies, output areas of *apterous-Gal4* neurons seem to accumulate within the longitudinal median fascicle, whereas the variable and construct-dependent localization along the transverse primary neurite is more likely to represent extrasynaptic surplus protein. Hence, Gal4-based visualization of synapses has the potential to be used in combination with genetic or experimental manipulations or for mutational screens.

What might be the mechanisms of compartmentalization?

On the one hand, mechanisms involved in the compartmentalization of output synapses along neurites must depend on intracellular components organizing the cortical cytoskeleton. Indeed, in *Drosophila* motoneurons, presynaptic structures can assemble in the absence of extracellular contacts (i.e., without postsynaptic muscles), demonstrating the existence of cell-autonomous mechanisms (Prokop et al., 1996). At NMJs, Kakapo seems to represent such an intrinsic factor because there are strong indications that Kakapo functions cell autonomously (Prokop et al., 1996; Lee and Luo, 1999). However, *kakapo* mutant alleles affecting NMJ differentiation failed to demonstrate a similar requirement of Kakapo for the number and localization of CNS output synapses (Fig. 6). This indicates potential differences of synaptogenetic mechanisms in the CNS and at NMJs. Such an scenario would not be unlikely, given the fact that most central synapses are cholinergic or GABAergic, whereas NMJs are glutamatergic (Johansen et al., 1989; Takagawa and Salvaterra, 1996; our unpublished results). Also in vertebrates, developmental mechanisms seem to differ at central and neuromuscular synapses (Serpinskaya et al., 1999).

Intracellular components required for the distribution of output synapses might be (partially) orchestrated by extracellular cues (Suter and Forscher, 2001). Thus, in the absence of such extrinsic cues, synapses might be formed but mislocalized. A paradigm for response of intrinsic synapse assembly mechanisms to extracellular cues was established in hippocampal cell cultures where axonal transport vesicles carrying various presynaptic proteins get trapped at points of contact with dendrites, thus seeding new output synapses (Ahmari et al., 2000). In contrast to randomly provided signals in cell culture, extrinsic signals in the stereotypically structured CNS could be provided in an ordered manner. This could explain the reproducible localization of output synapses that we observed. Cell cultures for *Drosophila* in which extrinsic versus intrinsic mechanisms can be tested are established in our laboratory and presently analyzed in this context (unpublished observations).

One attractive thought is that mechanisms patterning the CNS during earlier development might have an impact on the distribution of output synapses. For example, cell-surface molecules involved in pathfinding aspects in grasshoppers or *Drosophila* seem to be compartmentalized during earlier development (Goodman and Doe, 1993; Rajagopalan et al., 2000), and mechanisms underlying compartmentalization of output synapses might be related to these mechanisms. No mechanisms of compartmentalization have been identified so far, but *Drosophila* provides efficient tools and techniques to address them.

REFERENCES

Ahmari SE, Buchanan J, Smith SJ (2000) Assembly of presynaptic active zones from cytoplasmic transport packets. Nat Neurosci 3:445–451.

Blagburn JM, Alexopoulos H, Davies JA, Bacon JP (1999) A null mutation in *shaking-B* eliminates electrical, but not chemical, synapses in the *Drosophila* giant fibre system: a structural study. J Comp Neurol 404:449–458.

Bossing T, Technau GM (1994) The fate of the CNS midline progenitors in *Drosophila* as revealed by a new method for single cell labeling. Development 120:1895–1906.

Bossing T, Udolph G, Doe CQ, Technau GM (1996) The embryonic CNS lineages of *Drosophila melanogaster.* I. The lineages derived from the ventral half of the truncal neuroectoderm. Dev Biol 179:41–64.

Brand A, Perrimon N (1993) Targeted gene expression as a means of altering cell fates and generating dominant phenotypes. Development 118:401–415.

Broadie KS (2000) Electrophysiological approaches to the neuromusculature junction. In: *Drosophila* protocols (Sullivan W, Ashburner M, Hawley RS, eds), pp 273–295. Cold Spring Harbor, NY: Cold Spring Harbor Laboratory.

Budnik V, Gramates LS (1999) Neuromuscular junctions in *Drosophila.* San Diego: Academic.

Burrows M (1996) The neurobiology of an insect brain. Oxford: Oxford UP.

Calleja M, Moreno E, Pelaz S, Morata G (1996) Visualization of gene expression in living adult *Drosophila.* Science 274:252–255.

Doe CQ, Technau GM (1993) Identification and cell lineage of individual neural precursors in the *Drosophila* CNS. Trends Neurosci 16:510–514.

Godenschwege TA, Pohar N, Buchner S, Buchner E (2000) Inflated wings, tissue autolysis and early death in tissue inhibitor of metalloproteinases mutants of *Drosophila.* Eur J Cell Biol 79:495–501.

Goodman CS, Doe CQ (1993) Embryonic development of the *Drosophila* central nervous system. In: The development of *Drosophila* (Bate M, Martínez-Arias A, eds), pp 1131–1206. Cold Spring Harbor, NY: Cold Spring Harbor Laboratory.

Greenspan RJ (1997) Fly pushing: the theory and practice of *Drosophila* genetics. Cold Spring Harbor, NY: Cold Spring Harbor Laboratory.

Hiesinger PR, Reiter C, Schau H, Fischbach K-F (1999) Neuropil pattern formation and regulation of cell adhesion molecules in *Drosophila* optic lobe development depend on synaptobrevin. J Neurosci 19:7548–7556.

Ito K, Suzuki K, Estes P, Ramaswami M, Yamamoto D, Strausfeld NJ (1998) The organization of extrinsic neurons and their implications in the functional roles of the mushroom bodies in *Drosophila melanogaster* Meigen. Learn Mem 5:52–77.

Johansen J, Halpern ME, Johansen K, Keshishian H (1989) Stereotypic morphology of glutamatergic synapses on identified muscle cells of *Drosophila* larvae. J Neurosci 9:710–725.

Killmann F, Gras H, Schürmann F-W (1999) Types, numbers and distribution of synapses on the dendritic tree of an identified interneuron in the brain of the locust. Cell Tissue Res 296:645–665.

Klagges BRE, Heimbeck G, Godenschwege TA, Hofbauer A, Pflugfelder GO, Reifegerste R, Reisch D, Schaupp M, Buchner S, Buchner E (1996) Invertebrate synapsins: a single gene codes for several isoforms in *Drosophila.* J Neurosci 16:3154–3165.

Landgraf M, Bossing T, Technau GM, Bate M (1997) The origin, location, and projection of the embryonic abdominal motoneurons of *Drosophila.* J Neurosci 17:9642–9655.

Lee T, Luo L (1999) Mosaic analysis with a repressible neurotechnique cell marker for studies of gene function in neuronal morphogenesis. Neuron 22:451–461.

Littleton JT, Bellen HJ, Perin MS (1993) Expression of synaptotagmin in *Drosophila* reveals transport and localization of synaptic vesicles to the synapse. Development 118:1077–1088.

Littleton JT, Stern M, Perin M, Bellen HJ (1994) Calcium dependence of neurotransmitter release and rate of spontaneous vesicle fusions are altered in *Drosophila synaptotagmin* mutants. Proc Natl Acad Sci USA 91:10888–10892.

Lundgren SE, Callahan CA, Thor S, Thomas JB (1995) Control of neuronal pathway selection by the *Drosophila* LIM homeodomain gene *apterous.* Development 121:1769–1773.

Luo L, Liao YJ, Jan LY, Jan YN (1994) Distinct morphogenetic functions of similar small GTPases: *Drosophila* Drac1 is involved in axonal outgrowth and myoblast fusion. Genes Dev 8:1787–1802.

Meinertzhagen IA, Sorra KE (2001) Synaptic organization in the fly's optic lamina: few cells, many synapses and divergent microcircuits. Prog Brain Res 131:53–69.

Peters A, Palay SL, Webster Hd (1991) The fine structure of the nervous system, Ed 3. Oxford: Oxford UP.

Prokop A (1999) Integrating bits and pieces: synapse formation in *Drosophila* embryos. Cell Tissue Res 297:169–186.

Prokop A, Technau GM (1991) The origin of postembryonic neuroblasts in the ventral nerve cord of *Drosophila melanogaster.* Development 111:79–88.

Prokop A, Technau GM (1993) Cell transplantation. In: Cellular interactions in development: a practical approach (Hartley D, ed), pp 33–57. London: Oxford UP.

Prokop A, Landgraf M, Rushton E, Broadie K, Bate M (1996) Presynaptic development at the *Drosophila* neuromuscular junction: the assembly and localisation of presynaptic active zones. Neuron 17:617–626.

Prokop A, Uhler J, Roote J, Bate MC (1998) The *kakapo* mutation affects terminal arborisation and central dendritic sprouting of *Drosophila* motorneurons. J Cell Biol 143:1283–1294.

Rajagopalan S, Vivancos V, Nicolas E, Dickson BJ (2000) Selecting a longitudinal pathway: Robo receptors specify the lateral position of axons in the *Drosophila* CNS. Cell 103:1033–1045.

Rao A, Cha EM, Craig AM (2000) Mismatched appositions of presynaptic and postsynaptic components in isolated hippocampal neurons. J Neurosci 20:8344–8353.

Robertson HM, Preston CR, Phillis RW, Johnson-Schlitz DM, Benz WK, Engels WR (1988) A stable genomic source of P element transposase in *Drosophila melanogaster.* Genetics 118:461–470.

Robinson IM, Ranjan R, Schwarz TL (2002) Synaptotagmins I and IV promote transmitter release independently of Ca^{2+} binding in the C(2)A domain. Nature 418:336–340.

Schmid A, Chiba A, Doe CQ (1999) Clonal analysis of *Drosophila* embryonic neuroblasts: neural cell types, axon projections and muscle targets. Development 126:4653–4689.

Schmidt H, Rickert C, Bossing T, Vef O, Urban J, Technau GM (1997) The embryonic central nervous system lineages of *Drosophila melanogaster.* II. Neuroblast lineages derived from the dorsal part of the neuroectoderm. Dev Biol 198:186–204.

Schrader S, Merritt DJ (2000) Central projections of *Drosophila* sensory neurons in the transition from embryo to larva. J Comp Neurol 425:34–44.

Serpinskaya AS, Feng G, Sanes JR, Craig AM (1999) Synapse formation by hippocampal neurons from Agrin-deficient mice. Dev Biol 205:65–78.

Spradling AC, Rubin GM (1982) Transposition of cloned P elements into *Drosophila* germ line chromosomes. Science 218:341–347.

Südhof TC, Scheller RH (2001) Mechanisms and regulation of neurotransmitter release. In: Synapses (Cowan WM, Südhof TC, Stevens CF, Davies K, eds), pp 177–216. Baltimore: Johns Hopkins UP.

Suter DM, Forscher P (2001) Transmission of growth cone traction force through apCAM-cytoskeletal linkages is regulated by Src family tyrosine kinase activity. J Cell Biol 155:427–438.

Takagawa K, Salvaterra P (1996) Analysis of choline acetyltransferase protein in temperature sensitive mutant flies using newly generated monoclonal antibody. Neurosci Res 24:237–243.

Thomas JB, Bastiani MJ, Bate M, Goodman CS (1984) From grasshopper to *Drosophila*: a common plan for neural development. Nature 310:203–206.

Udolph G, Prokop A, Bossing T, Technau GM (1993) A common precursor for glia and neurons in the embryonic CNS of *Drosophila* gives rise to segment-specific lineage variants. Development 118:765–775.

vanVactor DV, Sink H, Fambrough D, Tsoo R, Goodman CS (1993) Genes that control neuromuscular specificity in *Drosophila.* Cell 73:1137–1153.

Vosshall LB, Wong AM, Axel R (2000) An olfactory sensory map in the fly brain. Cell 102:147–159.

Zinsmaier K, Hofbauer A, Heimbeck G, Pflugfelder G, Buchner S, Buchner E (1990) A cysteine-string protein is expressed in retina and brain of *Drosophila.* J Neurogenet 7:15–29.